

Influence of carbon black trimodal mixture on LDPE films properties: Part1 – DOE

Juliano Martins Barbosa^{1,2*} , Cesar Augusto Gonçalves Beatrice¹  and Luiz Antonio Pessan¹ 

¹Programa de Pós-graduação em Ciência e Engenharia de Materiais – PPGCEM, Departamento de Engenharia de Materiais – DEMa, Universidade Federal de São Carlos – UFSCar, São Carlos, SP, Brasil
²Engenharia de Materiais, Escola de Engenharia, Universidade Presbiteriana Mackenzie, São Paulo, SP, Brasil
*juliano.barbosa@mackenzie.br

Abstract

In this study, the influence of carbon black (CB) trimodal mixture, with different medium particle sizes, on the colorimetric and rheological properties of polyethylene was evaluated. Three different types of CB were selected, with particle sizes of 15nm (S), 38nm (M), and 75nm (L) and combined, generating a Design of Experiments (DOE) with 19 formulations to be dispersed at 30% in low density polyethylene (LDPE) in twin screw extruder. Such formulations were evaluated in performance and process properties, such as Tint Strength, Melt Flow Index (MFI), and Total Transmittance (TT). It was observed that the mixtures between small (S) and medium (M) particles developed greater tinting strength and lower viscosity, demonstrating the synergy of the mixture, which was superior in the performance of the mixture containing only a particular of 15nm (S) that would have greater potential for results.

Keywords: carbon black, polyethylene, tinting strength, trimodal particle size distribution, viscosity.

How to cite: Barbosa, J. M., Beatrice, C. A. G., & Pessan, L. A. (2022). Influence of carbon black trimodal mixture on LDPE films properties: Part1 – DOE. *Polímeros: Ciência e Tecnologia*, 32(3), e2022029. <https://doi.org/10.1590/0104-1428.20220039>

1. Introduction

Polymers are organic macromolecules (synthetic or natural origin). Plastics and rubbers are examples of synthetic polymers, while leather, silk, horn, cotton, wool, wood and natural rubber are natural organic macromolecules. They generally have low density, electrical and thermal insulation, flexibility, good corrosion resistance and low heat resistance^[1]. Synthetic polymers are produced by the polymerization of smaller molecules (monomers) in a process called polymerization, and most of their properties derive from this operation; however, they can be modified and improved by the addition of small amounts of additives or larger amounts in the case of mineral fillers^[2,3].

Thus, using the Principle of Combined Action, obtaining a multiphase material that has a significant proportion of the properties of both phases that constitute it in order that a better combination of the properties of the individual materials is obtained. Furthermore, the constituent phases must be chemically distinct and separated by an interface^[2].

An example of this is the addition of fillers in the polymer matrix, such as carbon black (CB) or calcium carbonate (CaCO₃), which can give the polymer better mechanical properties under tensile or impact, change the optical properties and reduce the cost of the product. The CB is used to develop mainly polymer reinforcements, especially elastomers, providing substantial mechanical strength^[4,5].

Although produced since remote antiquity, it only began to be manufactured industrially from 1870 onwards

to meet the needs of the paint industry. The discovery of its reinforcing properties in rubber, which took place in the early 20th century, raised this product to the current status of an essential filler for this industry, being even indispensable in many other applications.

The term reinforcement in polymer technology means an increase in mechanical performance, mainly in tear, tensile and abrasion resistance^[6]. The effect on the dynamic properties of elastomers differs quantitatively from one elastomer to another. It depends on the type of processing and the state of dispersion, both concerning the size and number of agglomerates and the separation distance between them^[5]. In addition to its wide use as a reinforcing agent in rubber, it can be used as a coloring agent for pigmentation, providing protection from UV radiation, increasing the electrical conductivity of the matrix but altering the rheological properties of polymers inks and coatings^[6]. These properties change with the morphology of the particles and are arranged in: particles, aggregates and agglomerates, as illustrated in Figure 1a^[7]. The particle is the primary spherical unit, characterized by its surface area, measured by Nitrogen Absorption (NSA) and expressed in m²/g^[6,7]. The Aggregate refers to a set of primary particles covalently bonded and represents the fundamental structure of CB suspension. These aggregates are defined by their Oil Absorption value (OAN) and expressed in cm³/100g. They often assume various arrangements such as spheroid, ellipsoidal, linear and super-branched. Finally, the Agglomerate (cluster)

is a group of aggregates linked through secondary bonds. The magnitude of this binding force can change with the chemical properties of the particles, the suspension vehicle, and the shape and size of the agglomerates. This structural change is sensitively perceived through the rheological responses of the suspensions. In general, an increase in CB concentration and a decrease in particle size improve and even prevent the formation of agglomerates, thus increasing viscosity^[6,7].

Concerning the optical properties developed by the tinting strength of the pigment, these are related to the size of the Primary Particle; that is, the smaller the particle, the greater the total surface area and the more intense the coloration developed. At this point, there is a conflict because the highest possible yield of coloring is desired. For that, a small primary particle is needed and preferably with a small aggregate structure to influence little on the viscosity of the matrix, thus enabling processing under normal conditions, i.e., the use of small particles allows for greater colorimetric yield. However, their use tends to increase the viscosity of the polymer significantly, which causes processing difficulties. Thus, the mixture of particles can be used to develop synergy between different particle sizes and minimally influence the increase in the viscosity of the matrix, using a packing with multimodal particle distribution^[8], contributing to the development of information and knowledge on the CB application, mainly in polyethylene, with the objective of acting as a colorant, in order to increase this property as much as possible, without affecting the rheological characteristics of the polymer and consequently its industrial processability. This study can contribute significantly to the industry, as such research is extremely complex, as the works on particle packing are well developed in the ceramic segment, but it is not yet used in mixing different particles of CB, in order to increase the tinting strength of the formulation. So, the challenge is to enable the use of pigment concentrates (masterbatch), produced with mixtures of different CB types, using different particle sizes in order to improve

the colorimetric properties of polyethylene used for the production of different products such as films, sheets or parts. With this, an improvement in the optical properties is expected, with greater tinting strength capacity, and with little influence on the rheological properties.

2. Materials and Methods

2.1 Materials

The inorganic pigment (Carbon black - CB) was identified as Black Pearls 900 (Small - S), Regal 991 (Medium - M) and Black Pearls 120 (Large - L), all supplied by Cabot Corporation (USA), according to Table 1^[9] and dispersed at 30% loading in low density polyethylene (LDPE) grade PB608^[10], with MFI of 30 g/10min (2.16 kg@190 °C) or 65 g/10min (5.00 kg@190 °C) produced by Braskem (Brazil).

2.2 Carbon black concentrates preparation

The pigment concentrates were dispersed in a twin-screw extruder ZSK18 (Coperion GmbH) with L/D 48, using screw rotation of 300 rpm (N), feed rate of 20 kg/h (Q) and a thermal profile between 120 and 180 °C, according to DOE Simplex Lattice Grade 4 shown in Figure 1b. The screw extruder profile was based on the scheme shown in Figure 2, however, there was a need for small adaptation due to the difference in L/D between the extruders^[11]. The pigments, supplied in the micro-pearls form, were manually homogenized with polyethylene pellets and then the mixture was dosed through the main feeder, using the flow rate previously indicated (Q).

The samples in this step, called PART 1, were identified with the following nomenclature: FXX(S/M/L), indicating the correlation between name and composition. For example, the formula F01 was identified as F01(75/25/00), with 75% of the total fraction of CB with S particle, 25% of M particle and 00% of L particle. The total CB content defined was 30%; for F01, we will have 75% x 30% and 25% x 30%, resulting in 22.5% for S and 7.5% for M, in addition to 70% of polyethylene, completing the composition.

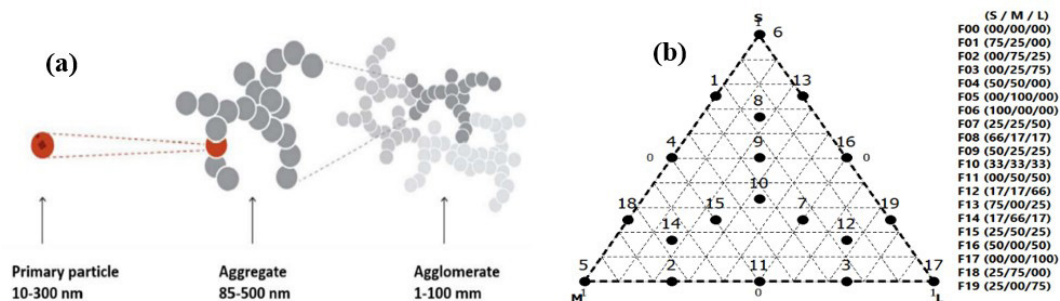


Figure 1. (a) Carbon Black morphology; (b) design of experiment.

Table 1. Principal properties of carbon black^[9].

Properties	Unit	Standard	BP 900 (S)	Regal 991 (M)	BP 120 (L)
Primary particle	nm	ASTM D3849	15	38	75
Oil absorption (OAN)	cc/100g	ASTM D2414	64	63	64
Nitrogen Surface Area (NSA)	m ² /g	ASTM D6556	230	62	25
Tinting Strength	%	ASTM D3265	151	97	58

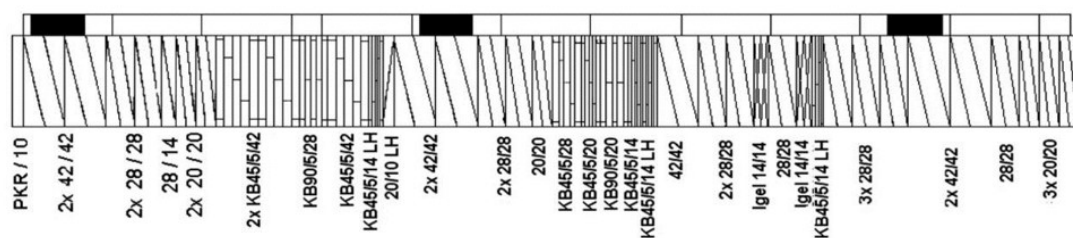


Figure 2. Schematic representation of the screw profile.

2.3 Dilution of carbon black concentrates

For some tests, the measures were in a polymeric film, and the specimens were prepared by blow mold extrusion (thickness 40 μm and blowing ratio of 1:3) diluting the concentrate at 5% in LDPE (MFI of 2 g/10min) in a single-screw, model D-85560 Ebersberg (Dr. Collin GmbH) with L/D 30 and D=25mm,

2.4 Characterizations

2.4.1 Composition characterization

The CB content in the samples was determined via gravimetric after pyrolysis at 600 $^{\circ}\text{C}$ in an inert nitrogen atmosphere and then in a regular atmosphere, following the ASTM D1603^[12].

2.4.2 Rheological properties characterization of carbon black concentrates

The MFI, which is a basic determination of the rheological behavior of compositions, was determined according to ASTM D1238 (5.00 kg@190 $^{\circ}\text{C}$)^[13]. Subsequently, the rheological properties were determined at low shear rates (steady flow regime) and high shear rates. The viscosity (η) as a function of shear rate ($\dot{\gamma}$) in steady flow regime was determined in a rheometer ARES from Rheometric Scientific (N_2 atmosphere, 210 $^{\circ}\text{C}$, parallel plates geometry with a diameter of 25 mm and 1 mm of gap) with a shear rate between 10^{-2} and 10^2 s^{-1} . The behavior at high shear rates was obtained by capillary rheometry in an Instron rheometer, model 4467 ($L_c = 24.384 \text{ mm}$, $D_c = 1.270 \text{ mm}$, $L_c/D_c = 20$ at 210 $^{\circ}\text{C}$) with a shear rate range between 10^1 and 10^4 s^{-1} which is equivalent to the values found in a twin-screw extrusion process^[14].

2.4.3 Colorimetric and optical properties characterization

The Tinting Strength is a quantitative method for comparing pigment performance to a reference. Prepared by mixing one part of CB concentrate (black) with ten parts of titanium dioxide pigment (white) – 1:10, generating a gray color. The more intense this gray, the greater the tinting strength of CB, as it stands out over white. On the other hand, the less intense the gray, the lesser the tinting strength because the white pigment stands out from the CB. The quantitative determination was performed in a spectrophotometer Datacolor (SF 600), using the “Contrast Ratio” mode, calculated by the CIE LAB L^*a^*b system^[15]. For Total Transmittance (TT), measured in a film specimen, which physically represents the total incident light and transmitted through the sample,

being reduced by the reflectance or absorption of light by the sample, measured using a BYK Gardner spectrophotometer (Haze-Gard Plus), following ASTM D1003 standard, operating in transmittance mode^[16-18].

2.4.4 Dispersion and microscopy characterization

The state of the dispersion was evaluated by two techniques: the first (quantitative) via Filter Pressure Value (FPV) and the second (qualitative) by Optical Microscopy (OM), observing the agglomerates dispersed in the polymer matrix. The FPV evaluates the degree of dispersion of pigments through a standardized screen filtration mounted on an extruder; this filtration generates retention of undispersed pigment particles, and the degree of dispersion can be quantified by the pressure variation, according to EN-13900^[19], using #635 mesh (15 μm), 220 $^{\circ}\text{C}$ and 200 g of concentrate. The FPV in the OM observed the CB microdispersion in the films specimen using a Leica microscope (DMRXP) and images captured with Image Pro Software at 200 or 400x magnification.

3. Results and Discussions

In PART 1 (Preliminary Formulation), the objective was to obtain the best proportion between the different CBs dispersed in a twin-screw extruder, resulting in the best dispersion with the highest possible tinting strength and maintaining the lowest viscosity. Table 2 shows the results of the characterizations, and its comprehensive evaluation indicates the most suitable combination and proportion between the pigments studied.

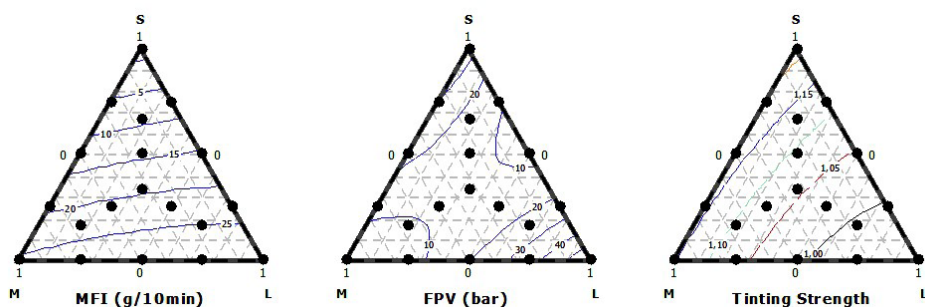
Table 2 shows that the CB content in the concentrates is within the expected range, which indicates that there was no significant loss or variation during the incorporation step. The nominal value of 30% ranged between 29.1% and 30.1%, with less than 3% in losses.

Assessing the properties of MFI, Tinting Strength and FPV, it is possible to observe the balance between the colorimetric properties and viscosity of the mixture, as shown in Figure 3 in the form of the Mixture Contour Graph.

The MFI showed that LDPE PB608, identified as **F00 (00/00/00)**, initially had 65.0 g/10min (5.00 kg@190 $^{\circ}\text{C}$), and its value was reduced to 0.80 g/10min for **F06 (100/00/00)** after the addition of small particles of CB, indicating a high increase in its viscosity. This behavior was already expected due to the capacity of the CB pigment to absorb the polymer and influence its viscosity, as presented by

Table 2. Results of the main characterization tests.

FXX (S/M/L)	S (%)	M (%)	L (%)	CB content (%)	MFI (g/10min)	Tinting Strength (%)	Ref. (F17)	Result	FPV (bar)	TT (%)
F00 (00/00/00)	0.00	0.00	0.00	0.00	65.0	0.00		-	0	82.7 ± 1.0
F01 (75/25/00)	22.5	7.50	0.00	29.5	5.40	113.0			68	9.7 ± 0.6
F02 (00/75/25)	0.00	22.5	7.50	29.7	26.9	109.0			21	11.3 ± 0.6
F03 (00/25/75)	0.00	7.50	22.5	28.9	28.5	96.90			33	15.5 ± 1.1
F04 (50/50/00)	15.0	15.0	0.00	29.1	12.3	114.1			8	10.8 ± 0.6
F05 (00/100/00)	0.00	30.0	0.00	29.6	26.1	109.8			1.5	9.7 ± 0.7
F06 (100/00/00)	30.0	0.00	0.00	30.0	0.80	124.5			21	6.1 ± 0.7
F07 (25/25/50)	7.50	7.50	15.0	30.1	23.1	102.7			13	13.2 ± 0.8
F08 (66/17/17)	20.0	5.00	5.00	30.2	6.80	111.1			7	11.4 ± 0.3
F09 (50/25/25)	15.0	7.50	7.50	29.7	14.2	106.4			8	12.5 ± 0.4
F10 (33/33/33)	10.0	10.0	10.0	29.6	20.9	109.2			13	15.2 ± 0.5
F11 (00/50/50)	0.00	15.0	15.0	29.7	28.6	100.6			13	18.5 ± 0.6
F12 (17/17/66)	5.00	5.00	20.0	29.8	26.6	95.30			21	18.9 ± 1.0
F13 (75/00/25)	22.5	0.00	7.50	29.7	4.60	113.9			14	12.4 ± 0.5
F14 (17/66/17)	5.00	20.0	5.00	30.0	23.3	106.6			13	16.2 ± 0.5
F15 (25/50/25)	7.50	15.0	7.50	29.9	21.8	110.5			12	15.1 ± 0.9
F16 (50/00/50)	15.0	0.00	15.0	29.9	14.2	106.6			13	16.1 ± 0.7
F17 (00/00/100)	0.00	0.00	30.0	29.9	27.9	100.0			62	17.0 ± 0.7
F18 (25/75/00)	7.50	22.5	0.00	30.0	18.8	126.7			1.2	7.2 ± 0.5
F19 (25/00/75)	7.50	0.00	22.5	29.6	26.3	97.10			26	16.8 ± 0.7

**Figure 3.** Mixture Contour Graph of MFI, FPV and Tinting Strength.

Zhang et al.^[20]. As reported in Table 1, there is a significant difference between the surface areas of the pigments, and this directly reflects on this result. Thus, pigment S with

a surface area of 230 m²/g (NSA) was the one that most affected this property and also in its combinations with pigment M, as in **F01 (75/25/00)**, which reduced it to 5.4 g/

10min or in **F08 (66/17/17)** with 6.80 g/10min pigment **L**, which has a smaller surface area, had less influence on this property, such as **F17 (00/00/100)** with 27.9 g/10min, as shown in Table 2.

The Tinting Strength, which determines pigment performance as a function of its ability to impart color to the polymer, can be evaluated considering the same amount of pigment mass in the formulations. This is due to the size of the primary particle and the structure of CB, which determine this property as a function of the surface area of the pigment. However, its degree of dispersion enhances this characteristic; the better it is dispersed, the greater the surface area of the pigment obtained and, consequently, the greater tinting strength, as widely discussed by Donnet^[21] and later by Spahr and Rothon^[22]. As this determination is comparative, **F17 (00/00/100)** was adopted as a reference (100%), as it was expected to be the one with the lowest because of the largest particle size in its composition

Again, the best results were obtained in compositions with pigments **S** and **M** and their combinations, such as **F06 (100/00/00)** with 124.5%, **F18 (25/75/00)** with 126.1% and **F04 (50/50/00)** with 114.1%. On the other hand, **F03 (00/25/75)** presented only 96.9%, this behavior as reported visually in Table 2 showing different grays and illustrated in Figure 3.

An important factor that influences the performance of the pigment in the polymer matrix is dispersion; in this way, the agglomerates are reduced during processing as a function of the shear, and the surface area of the pigment reaches its greatest potential; thus, the FPV provides a determination of the microdispersion of the pigment. The better its dispersion in the polymeric matrix, the lower the result because the agglomerates were reduced. The particles pass more easily through the filtering screen, not producing obstruction, consequently not increasing pressure. An important observation

is that the BP120 (**L**) pigment has a high level of impurities, which was not observed in the others, and this compromised the evaluation, as it was not possible to determine whether the increase in pressure was due to the poor dispersion of the pigment or the contaminants present in the raw material. Thus, the best results were obtained with pigments **S** and **M** and their combinations, as in **F17 (00/00/100)**, which presented 62 bar while **F03 (00/25/75)** and **F19 (00/25/75)** showed 33 bar and 26 bar, respectively.

Qualitatively the dispersion was observed by Optical Microscopy (OM). The agglomerates were identified, helping to understand the higher values of FPV due to the greater clogging and accumulation in the filtering screen^[19]. In Figure 4, some elements can be easily seen, such as the CB particles being well dispersed and some agglomerates, indicating a less efficient dispersion. Taking as reference **F17 (00/00/100)**, one can observe some extremes, such as **F18 (25/75/00)**, which showed good tinting strength (126.7%) and low FPV (1.2 bar) and also **F06 (100/00/00)** which showed good tinting strength (124.5%), slightly higher FPV (21 bar); however its micrograph showed the presence of many agglomerates, indicating poor dispersion and that it could have been better, enhancing the tinting strength, with reduced FPV. This fact is related to its large surface area, requiring greater Specific Mechanical Energy (SME) for complete dispersion due to its high viscosity^[22,23].

The formulations with pigment **S** showed a greater tendency to develop agglomerates, presenting points of poor dispersion, as in **F06 (00/00/100)**, **F01 (75/25/00)** and **F13 (75/00/25)**. On the other hand, the formulations containing pigment **L**, due to their structure, showed greater ease of dispersion and presented these poorly dispersed agglomerates in a reduced form, due to the combination with other pigments, as in **F17 (00/00/100)**, **F03 (00/25/75)**

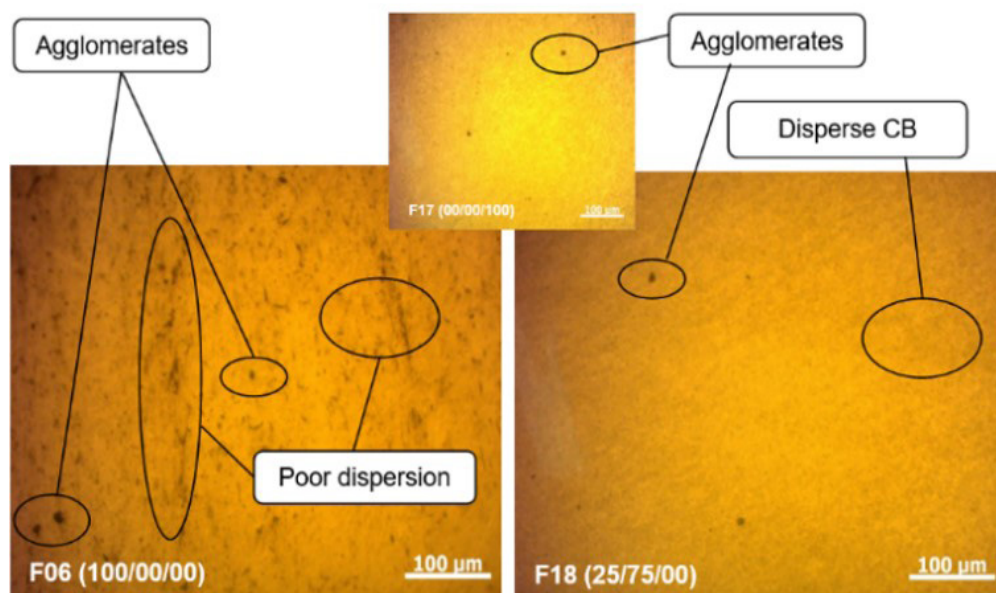


Figure 4. Micrographs of samples F06, F17 and F18 in MO (magnification: 200x).

and **F19 (00/25/75)**. The pigment **M**, which was expected to have an intermediate behavior, brought interesting results with good dispersion, as observed in **F05 (00/100/00)** and **F18 (25/75/00)**; this is due to its intermediate structure, which gives good dyeing power associated with less processing difficulty, in addition to less influence on viscosity, as shown in the Mixture Contour Graph of Figure 3 correlating these properties. This balance is essential as it provides sufficient viscosity to increase shear and enhance pigment dispersion without limiting processing due to excessive viscosity increase^[20]. In Figure 5, it is possible to see some of these micrographs at 400x magnification.

Correlating the Tinting Strength with the MFI, the Correlation Matrix was obtained for a preliminary and fundamental analysis of the balance between viscosity and performance, as shown in Figure 6a. It can be observed that some formulations are found in the quadrant with high tinting strength and higher MFI, such as **F01 (75/25/00)**, **F02 (00/75/25)**, **F04 (50/50/00)**, **F05 (00/100 /00)**, **F08 (66/17/17)**, **F10 (33/33/33)**, **F13 (75/00/25)**, **F15 (25/50/25)**

and **F18 (25/75/00)**. There is a strong tendency to reduce the MFI using **S** particle and its mixtures. However, this combination is the one that provided the greatest Tinting Strength; the **F18 (25/75/00)** presented a good balance between the properties, as demonstrated by Aghajan^[8].

Complementing the colorimetric evaluation, it was evidenced that the Total Transmittance (TT) measured in films has a strong correlation with the Tinting Strength, as shown in Table 2. The greater the tinting, the lower transmittance will be due to the pigment dispersed in the matrix; in addition to conferring the color, it also reduces the passage of light on the substrate, as observed in **F06 (100/00/00)**, **F13 (75/00/25)** and **F18 (75/25/00)**. Figure 6b shows this correlation more evidently.

The rheological behavior of the formulations was evaluated to complement the primary results from the MFI. The viscosity (η) as a function of shear rate ($\dot{\gamma}$) was measured, and some formulations presented higher viscosity than others as a function of their composition, as illustrated in Figure 7a, following the effect previously mentioned

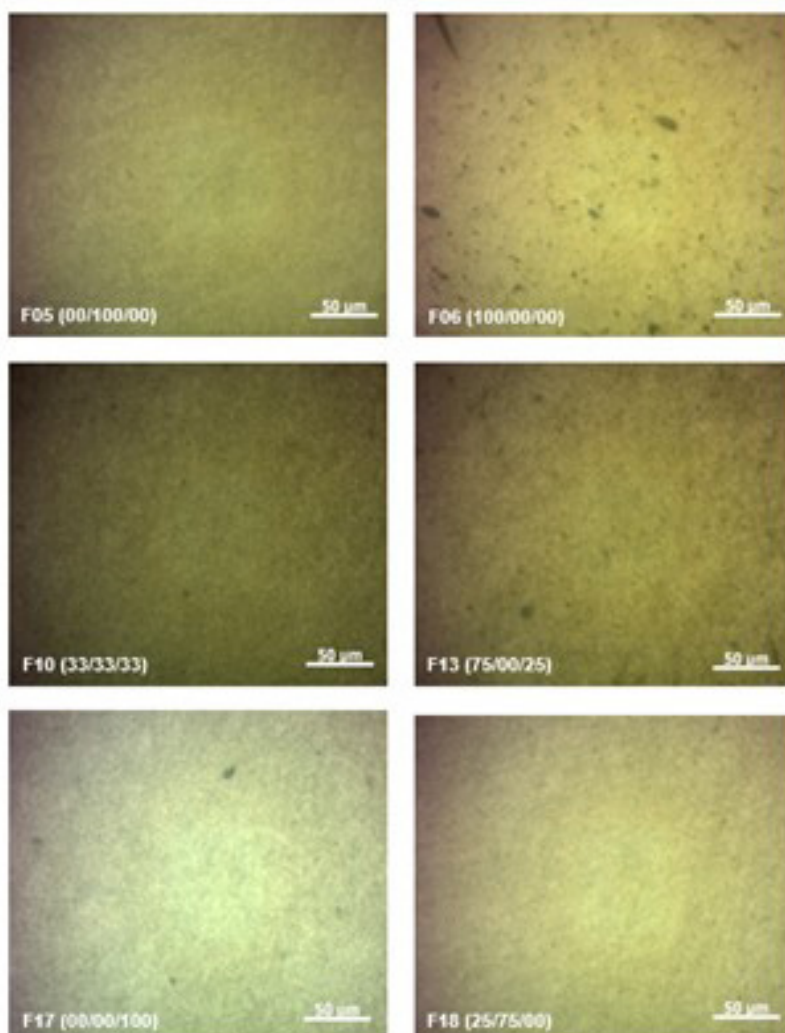


Figure 5. Micrographs of samples F05, F06, F10, F13, F17 and F18 in MO (magnification: 400x).

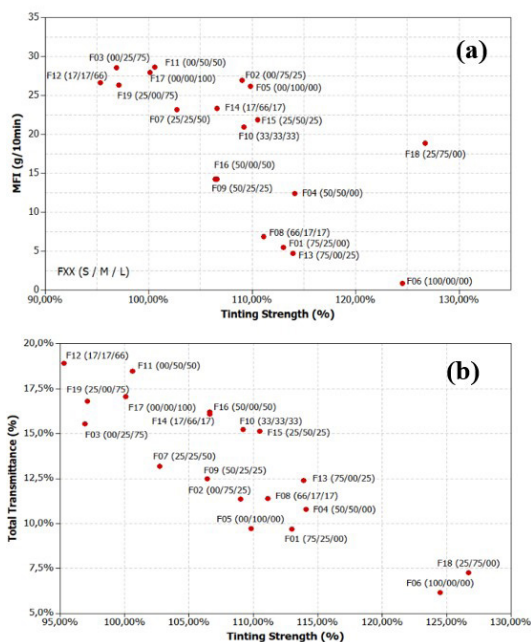


Figure 6. Correlation Matrix – (a) MFI and (b) Total Transmittance versus Tinting Strength.

on MFI behavior. In addition, the evaluation of $\eta(\dot{\gamma})$ also considers the pseudoplasticity of the polymer matrix^[14]. The rheological behavior as a function of composition, as expected, was influenced by the significant difference between the surface areas of the pigments. Thus, the pigment **S** with a surface area of 230 m²/g was the one that most affected the viscosity and also its combinations with the pigment **M**, such as **F06 (100/00/00)**, **F01 (75/25/00)**, **F04 (50/50/00)** that presented viscosity values in the order of 10⁵ Pa.s at a shear rate of 10⁻¹ s⁻¹. The formulation **F08 (66/17/17)** can be highlighted in the same order of magnitude. Pigment **L**, which has a smaller surface area, had less influence; for example, **F17 (00/00/100)** showed a viscosity value one order of magnitude lower at the same shear rate, as seen in Figure 7a. In this way, seeking the best balance between higher tinting strength with lower viscosity, the samples below were ordered from the lowest to the highest viscosity: **F17 (00/00/100) < F05 (00/100/00) < F18 (25/75/00) < F10 (33/33/33) < F13 (75/00/25) < F06 (100/00/00)**, such behavior observed by Chuayjuljit et al.^[24].

The rheological behavior at higher shear rates is essential to evaluate the pseudoplasticity at shear rates commonly applied to the polymer during processing^[14]. Thus, capillary rheometry was used to determine the viscosity as a function of shear rate, and the curves are shown in Figure 7b. Even at high rates, the rheological profile of viscosity remained close to 10³ s⁻¹, with **F06 (100/00/00)** being the highest viscosity and **F17 (00/00/100)** having the lowest values. Above this shear rate, the viscosity values are equivalent, and the curves overlap.

As determined by the previous tests, the **F06 (100/00/00)** showed high tinting strength; however, the viscosity also had high values. On the other hand, **F17 (00/00/100)** showed low viscosity values and did not develop tinting strength.

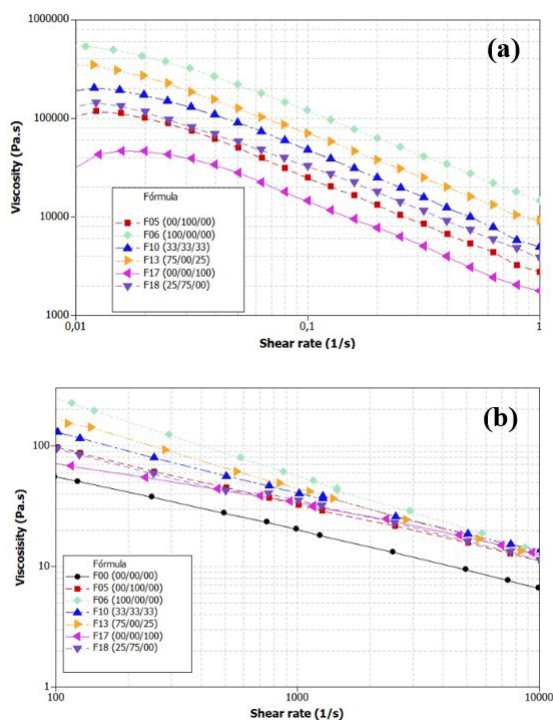


Figure 7. Viscosity as a function of shear rate for the best formulations balances measured at: (a) low shear rates (parallel plates); (b) high shear rates (capillary).

4. Conclusions

The trimodal mixture and distribution of different CB can produce an optimized combination between these pigments to improve the colorimetric properties, with less interference in the rheological and processing characteristics of the polymer, compared to using a single type of particle. The formulations containing small particle fractions (**S**) showed greater tinting strength and greater viscosity. The combinations showed superior performance than formulations containing only one type of particle. **F18 (25/75/00)** and **F13 (75/00/25)** had tinting power of 126.7% and 113.9%, respectively; the formulation **F17 (00/00/100)** was considered as 100%. The **F06 (100/00/00)**, which has only particles **P**, obtained 124.5% of tinting power due to its great difficulty in processing (high viscosity and consequent deficient dispersion). The viscosity results evaluated by the MFI show that **F00 (00/00/00)** went from 65 g/10min (5.00 kg@190 °C) to 18.8 g/10min in the formulation **F18 (25/75/00)** and 29.7 g/10min in the formulation **F13 (75/00/25)** while formulation **F06 (100/00/00)** reached 0.80 g/10min. The same behavior was observed in the rheological measurements. A factor that affects the performance of the pigment in the polymer matrix is its dispersion. The agglomerates are broken during processing due to the Specific Mechanical Energy (SME), providing better braking and dispersion of the agglomerates; thus, the surface area of the pigment reaches its highest values.

5. Author's Contribution

- **Conceptualization** – Juliano Martins Barbosa; Luiz Antonio Pessan.
- **Data curation** – Juliano Martins Barbosa; Luiz Antonio Pessan.
- **Formal analysis** – Juliano Martins Barbosa; Cesar Augusto Gonçalves Beatrice; Luiz Antonio Pessan.
- **Funding acquisition** – NA.
- **Investigation** – Juliano Martins Barbosa; Luiz Antonio Pessan.
- **Methodology** – Juliano Martins Barbosa; Cesar Augusto Gonçalves Beatrice; Luiz Antonio Pessan.
- **Project administration** – Juliano Martins Barbosa; Luiz Antonio Pessan.
- **Resources** – Juliano Martins Barbosa; Cesar Augusto Gonçalves Beatrice.
- **Software** – NA.
- **Supervision** – Juliano Martins Barbosa; Luiz Antonio Pessan.
- **Validation** – Juliano Martins Barbosa; Luiz Antonio Pessan.
- **Visualization** – Juliano Martins Barbosa; Luiz Antonio Pessan.
- **Writing – original draft** – Juliano Martins Barbosa; Luiz Antonio Pessan.
- **Writing – review & editing** – Juliano Martins Barbosa; Cesar Augusto Gonçalves Beatrice; Luiz Antonio Pessan.

6. Acknowledgements

This study was financed in part by the Coordenação de Aperfeiçoamento de Pessoal de Nível Superior - Brasil (CAPES) - Finance Code 001. The authors would like to thank the Engineering School of Mackenzie Presbyterian University, Cabot Corporation, Braskem S/A, and Cromex S/A for the technical support and donation of materials.

7. References

1. Padilha, A. F. (1997). *Materiais de engenharia: microestrutura e propriedades*. São Paulo: Hemus.
2. Callister, W. D., Jr. (2002). *Ciência e engenharia dos materiais: uma introdução*. Rio de Janeiro: LTC.
3. Wypych, G. (1999). *Handbook of fillers*. New York: ChemTec Publishing.
4. Darold, R. D. (2011). Influência da distribuição de tamanho de partículas sobre a piroplasticidade em porcelanato técnico em função do procedimento de moagem. *Cerâmica Industrial*, 16(3), 29-34. Retrieved in 2022, May 7, from <https://www.ceramicaindustrial.org.br/article/587657477f8c9d6e028b47a9>
5. Martins, A. F., Napolitano, B. A., Visconte, L. L. Y., & Nunes, R. C. R. (2002). Mechanical and dynamic mechanical properties of chloroprene rubber compositions with carbon black. *Polímeros: Ciência e Tecnologia*, 12(3), 147-152. <http://dx.doi.org/10.1590/S0104-14282002000300006>.
6. Aoki, Y., Hatano, A., & Watanabe, H. (2003). Rheology of carbon black suspensions. I. Three types of viscoelastic behavior. *Rheologica Acta*, 42(3), 209-216. <http://dx.doi.org/10.1007/s00397-002-0278-3>.
7. Carbon Black Association. (2016). *Carbon black user's guide*. USA: Carbon Black Association. Retrieved in 2022, May 7, from <http://www.cabotcorp.de/~media/files/product-stewardship/industry-user-guides/international-carbon-black-association-icba-user-guide-portuguese.pdf>
8. Aghajan, M. H., Hosseini, S. M., & Razzaghi-Kashani, M. (2019). Particle packing in bimodal size carbon black mixtures and its effect on the properties of styrene-butadiene rubber compounds. *Polymer Testing*, 78, 106002. <http://dx.doi.org/10.1016/j.polymertesting.2019.106002>.
9. Cabot Corporation. (2021, February 5). Retrieved in 2022, May 7, from <https://www.cabotcorp.com/solutions/applications/plastics>
10. Braskem. (2021, April 19). Retrieved in 2022, May 7, from <https://www.braskem.com/busca-de-produtos?p=133>
11. Lotti, C., Isaac, C. S., Branciforti, M. C., Alves, R. M. V., Liberman, S., & Bretas, R. E. S. (2008). Rheological, mechanical and transport property of blow films of high density polyethylene nanocomposites. *European Polymer Journal*, 44(5), 1346-1357. <http://dx.doi.org/10.1016/j.eurpolymj.2008.02.014>.
12. American Society for Testing and Materials – ASTM. (2020). *ASTM D1603-20: standard test method for carbon black content in olefin plastics*. West Conshohocken: ASTM. <http://dx.doi.org/10.1520/D1603-20>.
13. American Society for Testing and Materials – ASTM. (2013). *ASTM D1238-13: standard test method for melt flow rates of thermoplastics by extrusion plastometer*. West Conshohocken: ASTM. <http://dx.doi.org/10.1520/D1238-13>.
14. Bretas, R. E. S., & D'Ávila, M. A. (2000). *Reologia de polímeros fundidos*. São Carlos: EdUFScar.
15. Datacolor Color Measurement Instruments & Software. (2021, April 4). Retrieved in 2022, May 7, from <https://www.datacolor.com/business-solutions/product-overview>
16. Sarantópoulos, C. I. G. L., Oliveira, L. M., Padula, M., Coltro, L., & Alves, R. M. V. (2002). *Embalagens plásticas flexíveis: principais polímeros e avaliação das propriedades*. Campinas: CETEA/ITAL.
17. Byk Instruments. (2021, May 14). *Haze-gard transparency transmission haze meter*. Retrieved in 2022, May 7, from <https://www.byk-instruments.com/en/Appearance/haze-gard-Transparency-Transmission-Haze-Meter/c/2345>
18. American Society for Testing and Materials – ASTM. (2013). *ASTM D1003-13: standard test method for haze and luminous transmittance of transparent plastics*. West Conshohocken: ASTM. <http://dx.doi.org/10.1520/D1003-13>.
19. British Standards Institution – BSI. (2005). *BS EN 13900-5:2005: pigments and extenders: methods of dispersion and assessment of dispersibility in plastics - part 5: determination by filter pressure value test*. Belgium: BSI. <http://dx.doi.org/10.3403/30105254U>.
20. Zhang, J.-F., & Yi, X.-S. (2002). Dynamic rheological behavior of high-density polyethylene filled with carbon black. *Journal of Applied Polymer Science*, 86(14), 3527-3531. <http://dx.doi.org/10.1002/app.11101>.
21. Donnet, J.-B. (Ed.). (1993). *Carbon black: science and technology* (2nd ed.). New York: Routledge. <http://dx.doi.org/10.1201/9781315138763>.
22. Spahr, M. E., & Rotheron, R. (2015). *Carbon black as a polymer filler*. In S. Palsule (Ed.), *Encyclopedia of polymers and composites* (pp. 1-24). Berlin: Springer. http://dx.doi.org/10.1007/978-3-642-37179-0_36-1.

23. Domenech, T., Peuvrel-Disdier, E., & Vergnes, B. (2013). The importance of specific mechanical energy during twin screw extrusion of organoclay based polypropylene nanocomposites. *Composites Science and Technology*, 75, 7-14. <http://dx.doi.org/10.1016/j.compscitech.2012.11.016>.
24. Chuayjuljit, S., Imvittaya, A., Na-Ranong, N., & Potiyaraj, P. (2002). Effects of particle size and amount of carbon black and calcium carbonate on curing characteristics and dynamic mechanical properties of natural rubber. *Journal of Metals, Materials and Minerals*, 12(1), 51-57. Retrieved in 2022, May 7, from <https://www.jmmm.material.chula.ac.th/index.php/jmmm/article/view/1277/902>

Received: May 07, 2022

Revised: Aug. 20, 2022

Accepted: Sept. 21, 2022